Ribozyme-Mediated Cleavage of a Substrate Analogue Containing an Internucleotide-Bridging 5′-Phosphorothioate: Evidence for the Single-Metal Model†

Robert G. Kuimelis and Larry W. McLaughlin*

Department of Chemistry, Merkert Chemistry Center, Boston College, Chestnut Hill, Massachusetts 02167

Received December 19, 1995; Revised Manuscript Received February 19, 1996⊗

ABSTRACT: An oligonucleotide substrate containing a 5′-bridging phosphorothioate linkage adjacent to a ribonucleotide has been used to investigate the cleavage mechanism of the hammerhead ribozyme and to probe the catalytic role of the metal cofactor(s). Specifically, we tested the hypothesis that a second metal interacts with the 5′-leaving group to facilitate the cleavage event. To this end, we have examined the ribozyme-mediated cleavage activity of the phosphorothioate substrate at pH 7.5 with a series of divalent metals in both the presence and absence of the polycation spermine. The cleavage products are found to be the same as for the native sequence under a variety of reaction conditions. The influence of divalent metal ion concentration, temperature, and pH on the cleavage rate has also been examined for both the oxo linkage and the thio analogue. Spermine (but not spermidine or NaCl) is shown to support efficient cleavage of the thio analogue in the absence [5 mM ethylenediaminetetraacetic acid (EDTA)] of a divalent metal cofactor. The cleavage of the oxo linkage exhibits a solvent deuterium isotope effect of 3.6, but a similar effect is not observed with the thio analogue. The pseudo-first-order rate constants for cleavage of the thio analogue in the presence of 10 mM Mg^{2+} or Mn^{2+} at pH 7.5 are 65 and 82 $\times$ 10^{-3} min^{-1}, respectively. The native oxo linkage is cleaved at essentially the same rate as the thio analogue (35 and 97 $\times$ 10^{-3} min^{-1} for Mg^{2+} and Mn^{2+}, respectively). The absence of an appreciable thio effect and the lack of a preference for either Mg^{2+} or Mn^{2+} provides compelling evidence that the metal cofactor does not interact with the 5′-thioanion (or oxyanion) leaving group in the transition state. These rate comparisons additionally reveal that the departure of the 5′-leaving group is not the rate-limiting step of the cleavage reaction catalyzed by the hammerhead ribozyme.

Specific self-cleavage of RNA sequences in the absence of protein has been observed in a number of biological systems (Symons, 1991; Pyle, 1993). The hammerhead ribozyme is one such catalytic RNA that is derived from a structural motif present in the RNA genomes of several plant pathogens, where it is believed that the RNA-mediated cleavage events are an essential step in the viroid's replication pathway (Forster & Symons, 1987; Symons, 1989). The hammerhead ribozyme consists of three helical stems and includes nine conserved nucleotides (see Figure 1) that are nominally single-stranded and would appear to be responsible for the formation of a catalytically active domain (Forster & Symons, 1987; Uhlenbeck, 1987; Ruffner et al., 1990). Autolytic cleavage of a unique phosphodiester occurs via internal transesterification involving the 2′-hydroxyl adjacent to the scissile bond to generate fragments containing a terminal 5′-hydroxyl and a 2′,3′-cyclic phosphate (Uhlenbeck, 1987). Selected divalent metal ions are essential for efficient cleavage by the native ribozyme (Dahm & Uhlenbeck, 1991). The hammerhead ribozyme has been subjected to detailed kinetic analyses (Hertel et al., 1994; Long & Uhlenbeck, 1994; Hertel & Uhlenbeck, 1995). The relatively small size of the hammerhead complex, coupled with its ability to function *in trans*, makes this system amenable to chemical synthesis and a variety of informative experiments that are not possible in larger ribozyme systems. Recent structural studies (Heus & Pardi, 1991; Hodgson et al., 1994; Tuschl et al., 1994), including two crystal structures of hammerhead−inhibitor complexes (Pley et al., 1994; Scott et al., 1995), have provided a wealth of detailed information about the ground state conformation and have confirmed the main features of the early secondary structure predictions. Nucleoside analogue substitutions [reviewed in Kuimelis and McLaughlin (1996)] have identified specific functional groups on the heterocyclic and carbohydrate moieties that are critical for catalysis. Incorporation of phosphorothioates into the phosphate backbone has identified specific nonbridging phosphate oxygens involved in critical interactions

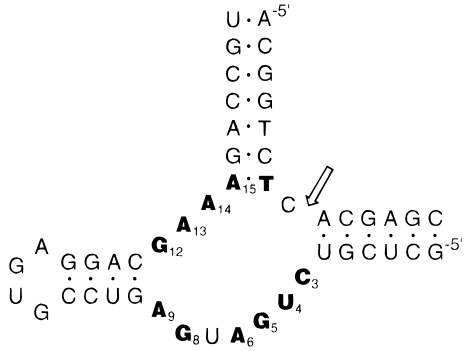

FIGURE 1: Sequence and secondary structure of the hammerhead ribozyme complex. The arrow indicates the cleavage site between positions C_{17} and $A_{1.1}$. Bold letters represent conserved nucleotides.

† This work was supported by a grant from the NIH (GM47660). L.W.M. is the recipient of an American Cancer Society Faculty Research Award (FRA-384).

* Author to whom all correspondence should be addressed.

⊗ Abstract published in *Advance ACS Abstracts,* April 1, 1996.

0006-2960/96/0435-5308$12.00/0

(Koizumi & Ohtsuka, 1991; Jeoung et al., 1994). Substitution of an isomerically pure phosphorothioate diester into the cleavage site and subsequent analysis of the cleavage products has confirmed that the reaction follows an in-line S_N2 mechanism with inversion of configuration at the phosphorus center (van Tol et al., 1990; Slim & Gait, 1991). Kinetic analyses of phosphorothioate-containing substrates have established that the *pro*-R (but not the *pro*-S) nonbridging oxygen of the scissile phosphodiester interacts with the metal cofactor in the transition state (Koizumi & Ohtsuka, 1991; Slim & Gait, 1991; Dahm et al., 1993). Solvated metal hydroxide has been implicated as the base responsible for the deprotonation of the 2′-hydroxyl and the initiation of cleavage (Dahm et al., 1993).

Although essentially considered to be metalloenzymes (Piccirilli et al., 1993; Pyle, 1993; Yarus, 1993), the precise role of the metal cofactor in the hammerhead ribozyme remains obscure. The exact number of metal atoms that are involved in the actual chemical cleavage event, or in the organization of the tertiary structure, remains to be clarified. The crystal structures (Pley et al., 1994; Scott et al., 1995) did not unambiguously identify the participating metals, although indirect methods were used to place a single hydrated Mg^{2+} atom near the cleavage site; a potential mechanism that involves this single metal was proposed (Scott et al., 1995). However, by analogy with several crystal structures of proteinacious phosphoryl transfer enzymes, where the roles of the metals have been clearly established, it has been proposed that a general two-metal mechanism may be operative (Freemont et al., 1988; Beese & Steitz, 1991; Steitz & Steitz, 1993). Gas-phase ab initio molecular orbital calculations of small model compounds have suggested that a second metal cofactor could function as a Lewis acid in the hammerhead ribozyme to stabilize the departing 5′-oxo leaving group and assist in the cleavage event (Taira et al., 1990, 1991; Uebayasi et al., 1994), but this hypothesis has not yet been proven (or disproven) experimentally.

To probe the cleavage mechanism of the hammerhead ribozyme and to investigate the possibility of a second metal cofactor, we have prepared an oligonucleotide containing an internucleotide 5′-bridging phosphorothioate diester adjacent to a ribonucleotide (Kuimelis & McLaughlin, 1995a,b) and compared the hammerhead-mediated substrate cleavage of the native and thio linkages under a variety of conditions, including the conventional condition of pH 7.5 and 10 mM divalent metal. This experiment was originally proposed by Slim and Gait (1991) and later elegantly applied to the group I intron by Cech and co-workers (Piccirilli et al., 1993) using an all-deoxy substrate containing a bridging 3′-phosphorothioate at the cleavage position. The substrates employed in the present study consist entirely of deoxynucleotides, except for the single mandatory ribonucleotide (C_{17}), and differ only in the nature of the phosphodiester bond at the cleavage site by the replacement of a single atom (i.e., oxygen vs sulfur). We have also characterized the products of each cleavage reaction and have investigated the influence of divalent metal ion type and concentration, polycations, temperature, and pH on the cleavage kinetics.

MATERIALS AND METHODS

General. Reagents and buffers were from Sigma or Aldrich Chemical Co. (Milwaukee, WI) and were used as supplied. High-performance liquid chromatography (HPLC) grade acetonitrile and methanol were from Fisher Scientific (Fair Lawn, NJ). Deoxynucleoside phosphoramidites and solid supports were from CPG, Inc. (Lincoln Park, NJ). Ribonucleoside phosphoramidites and solid supports were from Biogenex (San Ramon, CA). The Cee-protected cytidine phosphoramidite was a gift of Glen Research (Sterling, VA). Enzymes were from Boehringer (Mannheim, Germany) or New England Biolabs (Beverly, MA). [γ-^{32}P]-ATP was from NEN/DuPont (Wilmington, DE). Oligonucleotides were synthesized on an Applied Biosystems 381A DNA synthesizer. Fast protein liquid chromatography (FPLC) was performed with a Pharmacia FPLC system using a Mono-Q HR 10/10 strong anion exchanger column. HPLC was performed with a Beckman HPLC system using C-18 reversed-phase columns (ODS-Hypersil, 5 μm particle size, 120 Å pore, 4.6 × 250 mm). Chromatograms were recorded and quantitated with a Shimadzu C-R3A Chromatopac integrator. Electrophoresis gels were analyzed with a Molecular Dynamics Phosphorimager 425 and Image Quant v3.3 software.

Substrate Synthesis and Purification. The substrates were synthesized at 1 μmol scale using conventional β-cyanoethyl phosphoramidite methodology and long-chain alkylamine controlled-pore glass supports (500 Å pore size). The 5′-terminal dimethoxytrityl group was removed on the instrument (trityl off). Detritylations were performed with 2% dichloroacetic acid in anhydrous CH_2Cl_2. All oxidations were performed with the standard aqueous iodine/pyridine/THF mixture. The coupling time for the modified phosphoramidites was increased from 30 s to 9 min. After coupling, oxidizing, and capping of the 5′-thio nucleoside, the synthesis cartridge containing the support-bound oligonucleotide was removed from the instrument, washed with H_2O, and treated with $AgNO_3$ (50 mM, 3 mL) for 30 min in the dark to remove the triphenylmethyl group protecting the thiol. The cartridge was then thoroughly rinsed with H_2O, treated with dithiothreitol (50 mM, 3 mL) for 15 min, rinsed again with H_2O followed by acetonitrile, and finally dried in a vacuum desiccator for ca. 1 h. The cartridge, now containing a 5′-terminal thiol, was reattached to the synthesis instrument, and the next phosphoramidite (the specially protected 2′-Cee C monomer) was added, increasing the coupling time to 9 min. Subsequent phosphoramidite monomers were added in the conventional manner. After complete assembly of the oligonucleotide, the solid support was treated with concentrated NH_4OH (5 mL) at 50 °C for 12 h to release the oligomer from the support and remove the protecting groups. Sterile conditions were used from this point on when the oligomers were handled. Ammonia was removed under reduced pressure, and the oligomer was desalted with a Sephadex G-10 column (2 × 40 cm), eluted with H_2O, and lyophilized.

The crude oligonucleotide substrates were initially isolated and purified by anion-exchange chromatography using a Pharmacia FPLC system (10 mM KH_2PO_4, pH 6.35, and 30% acetonitrile with a KCl gradient). The optimum salt gradient for separation was 10 to 300 mM KCl over 13 min, followed by 300 to 400 mM KCl over 22 min at a flow rate of 1.5 mL/min. The full length 14-mer (5′-ACGGTCTrC-sACGAGC-3′) eluted at 360 mM KCl (25 min); the 12-mer disulfide (3′-CGAGCAs-sACGAGC-3′) eluted at 320 mM KCl (17 min), and the 8-mer fragment (5′-ACGGTCTrC) eluted at 270 mM KCl (12 min). The appropriate fractions

were collected, concentrated in vacuo, desalted on a Sephadex G-10 column, and lyophilized. The phosphorothioate oligomer was additionally purified by denaturing gel electrophoresis using 20% acrylamide, 7 M urea, and 1x TBE (pH 8.4) running buffer. The oligonucleotide was recovered by stirring the excised, crushed gel pieces in 300 mM NaOAc (pH 5.5) at 4 °C for 12 h. Buffers were removed by size exclusion chromatography with a Sephadex G-10 column. Some degradation of oligomer **2** (ca. 25%) occurred during electrophoresis at pH 8.4, so an additional FPLC purification and desalting was performed. Purified substrates were stored in solution at −20 °C.

Ribozyme Synthesis and Purification. The 35-mer ribozyme was chemically synthesized as described above for the substrates, but the phosphoramidite monomers contained *tert*-butyldimethylsilyl ether protecting groups at the 2′-hydroxyl position and phenoxyacetyl base protecting groups for G and A. Base deprotection was performed with anhydrous ammonia-saturated methanol (2.0 mL) for 12 h at ambient temperature. After being concentrated to dryness, the residue was taken up in 1.0 M TBAF/THF (1.0 mL) and shaken for 24 h in the dark. The solution was extracted with EtOAc (1.5 mL, three times) after addition of 3 M NaOAc (pH 5.8) (500 μL). The aqueous layer was concentrated in vacuo, desalted on a Sephadex G-10 column, and lyophilized to dryness. The crude, deprotected oligomer was purified by denaturing polyacrylamide gel electrophoresis (PAGE), extracted from the gel, and desalted as described above. The purified ribozyme was stored in solution at −20 °C.

Oligonucleotide Characterization. The 35-mer ribozyme was digested with S1 nuclease and alkaline phosphatase as previously described (Fu & McLaughlin, 1992) and gave the expected base composition results. For the 14-mer substrates, approximately 0.1 A_{260} unit was incubated overnight at 37 °C with snake venom phosphodiesterase (2 units) and alkaline phosphatase (2 units) in a total volume of 50 μL containing 100 mM Tris-HCl (pH 8.0) and 20 mM $MgCl_2$. A portion of this mixture was analyzed directly by reversed-phase HPLC using a 60 min linear gradient of 0 to 70% methanol in 20 mM KH_2PO_4 (pH 5.5). Detection was at 260 nm. The following correction factors were applied to the integrated areas of the nucleoside peaks to normalize the extinction coefficients: rC and dC, 7.8; dG, 12.5; dT, 8.4; dA and dsA, 13.1; and dAssA, 26. Retention times, in minutes, were as follows: rC, 4.0; dC, 5.7; dG, 10.7; dT, 11.7; dA, 15.3; dsA, 22.0; and dAssA, 34.4. Specific RNAse T_2 cleavage was performed on the substrates by treating the radiolabeled oligomer with 1 unit of RNAse T_2 at pH 4.5 (50 mM KH_2PO_4) for several hours. Gel electrophoresis revealed complete cleavage at the single ribonucleotide position.

Oligonucleotide Labeling. The substrates (ca. 200 pmol) were each end-labeled with [γ -^{32}P]ATP (15 μCi, 25 pmol) and T-4 polynucleotide kinase (30 units). Conventional conditions were used for the oxo linkage (i.e., 60 min at 37 °C, pH 7.6, 10 mM $MgCl_2$, and 10 mM 2-mercaptoethanol). The phosphorothioate analogue was end-labeled at 27 °C in the presence of 50 mM PIPES (pH 6.6), 1 mM $MgCl_2$, and 1 mM 2-mercaptoethanol; after 15 min, the reaction was quenched with 10 volumes of 50 mM PIPES (pH 6.6) and 10 mM ethylenediaminetetraacetic acid (EDTA). All the labeling reaction mixtures were applied to Sep-Pak C-18 columns, washed with 4% MeOH in H_2O (20 mL), eluted with CH_3CN/MeOH/H_2O (35:35:30, 4 mL), and lyophilized to dryness.

Cleavage Reactions. Two 20 μL solutions containing either 1 μM ribozyme or 1 nM radiolabeled substrate in 50 mM Tris-HCl (pH 7.5) were heated to 65 °C and slowly cooled to 27 °C (or the appropriate starting temperature) over 2 h. Ribozyme solutions were adjusted to 1 mM spermine (if indicated) and 20 mM metal dichloride (or 10 mM EDTA, added before heating); reactions were initiated by mixing of the two solutions. For the temperature studies, sample tubes were fully submerged in a thermostatted, circulating water bath. For the pH studies, the following sulfonic acid buffers were used in place of Tris: MES (pH 6.0), PIPES (pH 6.5), MOPS (pH 7.0), MOPS (pH 7.5), TAPS (pH 8.0), and TAPS (pH 8.5). Aliquots of 5 μL were withdrawn from the cleavage reaction mixture at appropriate time intervals, and the reaction was terminated by pipetting the aliquot into 1.5 volumes of gel loading solution and mixing. For the oxo substrate, the gel loading solution consisted of 50 mM EDTA, 7 M urea, 10% glycerol, 0.05% xylene cyanol, and 0.05% bromphenol blue; the solution for the thio analogue contained the same components but was buffered with 40 mM Tris-OAc (pH 6.8).

Electrophoresis. Conventional denaturing PAGE (20% acrylamide, 7 M urea, 18 × 16 × 0.1 cm) employing 1× TBE (pH 8.4) was used for the oxo substrate. For the thio analogue, the running buffer was 40 mM Tris, 20 mM NaOAc, and 1 mM EDTA at pH 6.8. Also, this buffer was recirculated between the upper and lower chambers with a peristaltic pump to maintain a constant pH throughout the run. The pH 6.8 gel was pre-electrophoresed for 2 h prior to the run, which was conducted at 10 mA for 8 h. Gels were exposed to a Kodak S0230 phosphor storage screen (Molecular Dynamics) for 12−24 h and were analyzed by phosphorimaging. First-order rate constants were calculated from the half-lives of the substrates ($k = 0.693/t_{1/2}$). The reported rate constants are an average of 2−5 kinetic experiments; standard deviations are no more than ±10% of the indicated value and in many cases are much less than ±10%.

Characterization of the Cleavage Products. Ribozyme cleavage products were separated by anion-exchange FPLC, and the fragments were subjected to quantitative nucleoside composition analysis using the previously described procedures. The cytidine 2′,3′-cyclic phosphate was identified by analysis of the digestion mixture on an anion-exchange HPLC column (APS-Hypersil, 5 μM particle size, 120 Å pore, 4.6 × 250 mm) with a 60 min linear gradient of 5 to 250 mM KH_2PO_4 (pH 6.3) + 5% CH_3CN. Under these conditions, the cytidine 2′,3′-cyclic phosphate eluted at 7.0 min and the 2′- and 3′-monophosphate standards eluted at 11.8 and 12.7 min, respectively.

The three electrophoresis standards (5′-fragment, ACGGTCTrC) were prepared as follows. The 2′,3′-dihydroxy rC oligonucleotide was chemically synthesized on a solid support employing 2′-OTBDMS protection. Deprotection was done with NH_4OH/EtOH followed by triethylamine trihydrofluoride. The 3′-phosphate rC oligonucleotide was prepared by digestion of 5′-^{32}P-labeled **1** with RNAse T_2 in KH_2PO_4 (50 mM, pH 4.5). The 2′,3′-cyclic phosphate rC oligonucleotide was prepared by digestion of 5′-^{32}P-labeled **1** with the ribozyme. The standards were purified by denaturing PAGE, excised, and extracted from the gel.

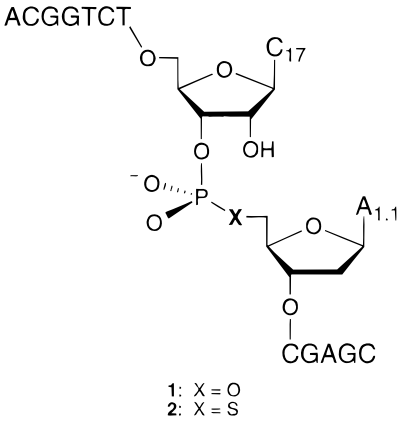

FIGURE 2: Illustration of the hammerhead substrates employed in this study, differing only in the nature of the phosphodiester bond between positions C_{17} and $A_{1.1}$.

Radiolabeled **2** was treated under each of the ribozyme cleavage conditions, in the presence of ribozyme, for an amount of time sufficient to cause >80% cleavage at the phosphorothioate linkage. Reactions were terminated by addition of EDTA to a final concentration of 10 mM, reduction of the volume, and addition of 20 μL of formamide. High-resolution electrophoresis (20% acrylamide, 7 M urea, and 1× TBE) was performed on a 27 cm × 80 cm × 0.4 mm gel run at 9 mA constant current for 12 h. Gels were dried and analyzed by phosphorimaging.

Solvent Isotope Effect Experiments. Solvent isotope effect experiments were carried out as described above for the normal ribozyme reaction, except stock solutions were prepared in either deuterium oxide (99.9 at. %) or 1:1 H_2O/D_2O (v/v). Ribozyme, substrate, and metal solutions were lyophilized from D_2O prior to dilution in the appropriate solvent. The pH of the D_2O-containing buffer solutions (Tris base) was adjusted with a DCl solution and was corrected according to the equation $pH = pD + 0.3139\alpha + 0.0854\alpha^2$, where α is the atom fraction of deuterium and pD is the reading obtained with a glass electrode (Pentz & Thornton, 1967). No adjustment was made for the protons released by the buffer.

RESULTS AND DISCUSSION

Design of the Substrates. The 14-mer DNA/RNA chimeric substrates (Figure 2) were chemically synthesized via conventional solid-supported phosphoramidite methodology (Matteucci & Caruthers, 1981) and were purified to homogeneity using electrophoresis and chromatographic methods. The sequences were designed with a single ribonucleotide at the cleavage site (C_{17}) and were sufficiently long to allow effective complex formation at 27 °C (the reaction temperature) despite the decreased stability of DNA/RNA heteroduplexes compared to that of RNA/RNA homoduplexes. The two sequences differ only in the nature of the phosphodiester bond between nucleotides C_{17} and $A_{1.1}$, where the 5′-bridging heteroatom is either oxygen (sequence **1**) or sulfur (sequence **2**). Predominantly deoxy substrates are effectively cleaved by the hammerhead ribozyme, albeit at a somewhat reduced rate, and behave very much like the all-ribo substrates (Dahm & Uhlenbeck, 1990; Perreault et al., 1990, 1991; Yang et al., 1990, 1992). The ribozyme sequence that we have employed in this study is identical to one reported earlier by Cedergren and co-workers; the ribozyme-mediated cleavage rate of **1** is about 10-fold less than that of the corresponding all-ribo sequence (Yang et al., 1990). Acid-labile acetal protection (Yamakage et al., 1989; Sakatsume et al., 1991a,b) was used for the single 2′-hydroxy position during assembly of the substrates due to the severe instability of the phosphorothioate linkage toward the conventional TBAF (Usman et al., 1987) and TEA-HF_3 (Gasparutto et al., 1992; Westman & Stromberg, 1994) reagents.

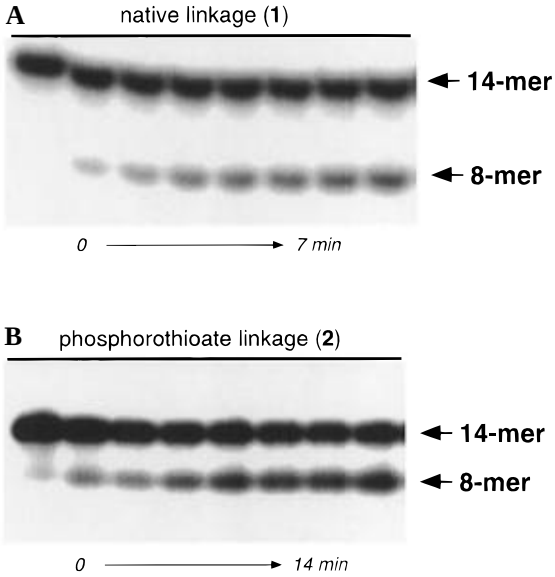

FIGURE 3: Representative gels showing the time course of product (8-mer) formation. (A) Hammerhead ribozyme-promoted cleavage (0−7 min) of the native oxo linkage; gel run at pH 8.4. (B) Hammerhead ribozyme-promoted cleavage (0−14 min) of the 5′-bridging phosporothioate linkage; gel run at pH 6.8.

Some modification of conventional procedures was required to minimize degradation of the phosphorothioate-containing substrate during preparation and analysis. For example, in addition to the normal precautions against nuclease contamination, special efforts were made to keep sequence **2** cold and to minimize the possible introduction of trace metals at all stages of manipulation. Enzymatic labeling of sequence **2** was done only briefly at 27 °C and pH 6.6, using one-tenth of the usual amount of Mg^{2+} and mercaptoethanol. Although these conditions are not optimal for the kinase enzyme and result in lower incorporation efficiencies, the changes were necessary to avoid substantial cleavage at the phosphorothioate linkage during the labeling reaction. Single-turnover conditions were employed to investigate the ribozyme-promoted cleavage kinetics of the oxo and thio linkages so that the observed rates would represent the actual chemical cleavage step. The ribozyme was always in large excess (1000-fold) over the substrate to assure that all of the substrate was hybridized with the ribozyme, where it is less susceptible to the effects of the solution-phase metal ions that contribute to background, non-ribozyme cleavage of the phosphorothioate linkage (vide infra). Figure 3 illustrates representative gels of the time course of product (8-mer) formation for both the oxo and thio linkages. It was necessary to perform electrophoresis of the thio substrate at pH 6.8 with buffer recirculation; the oxo substrate was electrophoresed at the conventional pH 8.4.

Analysis of the Cleavage Products. The normal products of the ribozyme reaction are 5′-hydroxy and 2′,3′-cyclic

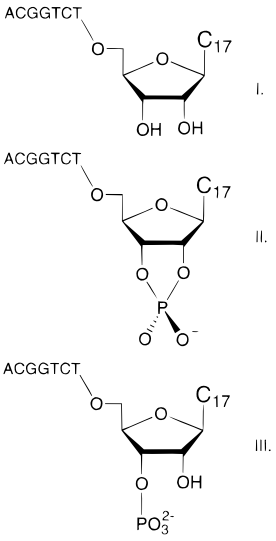

FIGURE 4: Possible 5′-fragments (8-mer) from the hammerhead ribozyme-promoted cleavage of the substrates illustrating the 3′-termini: (I) 2′,3′-dihydroxy, (II) 2′,3′-cyclic phosphate, and (III) 3′-phosphate.

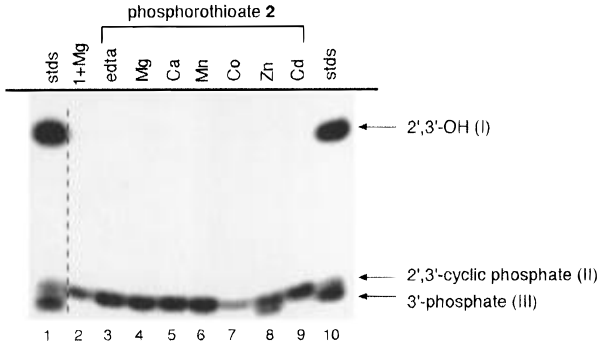

FIGURE 5: High-resolution PAGE analysis of the 5′-cleavage fragment (8-mer) from the hammerhead ribozyme-promoted cleavage of substrates under a variety of conditions. Lanes 1 and 10 (stds) are authentic standard controls containing a mixture of end-labeled 5′-ACGGTCTrC, where rC is 2′,3′-dihydroxy (I), 2′,3′-cyclic phosphate (II), or 3′-monophospate (III). See Figure 4 for structures. Lane 1 was from a different gel. Lane 2 is a control showing the 5′-cleavage fragment from the oxo linkage in the presence of Mg^{2+}. Lanes 3−9 show the 5′-cleavage fragment from the cleavage of the phosphorothioate analogue in the presence of EDTA/spermine or the indicated divalent metal.

phosphate-containing fragments (Uhlenbeck, 1987). A number of distinct cleavage pathways can be envisioned for the ribozyme-promoted cleavage of the bridging 5′-phosphorothioate substrate. The native cleavage mechanism involving transesterification by the 2′-hydroxyl generates a terminus containing the 2′,3′-cyclic phosphate. Two possible hydrolytic processes, one involving P−S bond cleavage and one involving P−O bond cleavage, result in termini containing the 3′-phosphate or the 2′,3′-diol, respectively. It was necessary to establish which pathway is operative for this substrate analogue, and this was accomplished by identification of the cleavage fragments. The possible 3′-termini for the 5′-cleavage fragment 5′-ACGGTCTrC are illustrated in Figure 4. Each of these possible products can be generated synthetically by chemical or enzymatic means, and the corresponding nucleotides are also readily available. The product fragments from the ribozyme-promoted cleavage of substrates **1** and **2** were isolated by ion-exchange chromatography and were subjected to enzymatic base composition analysis, which confirmed the site of cleavage and the presence of the rC 2′,3′-cyclic phosphate and the 5′-thio A (for the thio analogue). These results imply that the ribozyme-promoted cleavage of the bridging 5′-phosphorothioate substrate proceeds via the conventional transesterification pathway. To confirm that these same products are formed under a variety of conditions, we prepared authentic standards of the possible cleavage fragments and used high-resolution gel electrophoresis to evaluate the radiolabeled product (5′-fragment) of the ribozyme-promoted cleavage. The results are summarized in Figure 5. For each set of conditions that we examined, the reaction leads exclusively to the expected 2′,3′-cyclic phosphate (and presumably also generates a 5′-thiol terminus on the unlabeled 6-mer 3′-fragment). In the case of the ribozyme-promoted cleavage with Zn^{2+} as cofactor, a substantial amount of 3′(or 2′)-phosphate is also observed. However, control experiments with authentic standards revealed that this metal alone is capable of efficiently hydrolyzing the cyclic phosphate to the 2′(or 3′)-phosphate. It is therefore likely that in the ribozyme reaction the 2′,3′-cyclic phosphate is formed first and this product is subsequently hydrolyzed to the 2′(or 3′)-phosphate by the action of the Zn^{2+}. We have previously shown that the chemical cleavage of the bridging 5′-phosphorothioate in the absence of ribozyme can be accelerated by the presence of divalent metals and occurs via the same transesterification pathway under a variety of conditions (Kuimelis & McLaughlin, 1995a).

Effect of Divalent Metals. A series of divalent metals, each previously shown to individually stimulate the cleavage of all-ribo substrates (Dahm & Uhlenbeck, 1991), was examined for their ability to facilitate the ribozyme-promoted cleavage of the predominantly deoxy oxo and thio substrates. However, it was first necessary to establish the background (control) cleavage rates in the absence of ribozyme. The decreased pK_a of the mercapto versus that of the oxo group,[1] and the increased softness character of the sulfur atom make the 5′-bridging phosphorothioate linkage much more susceptible to cleavage than a conventional phosphodiester or a nonbridging phosphorothioate (Almer & Strömberg, 1991a,b) adjacent to a ribonucleotide. At pH 7.5 in the absence of metals (5 mM EDTA), the phosphorothioate linkage is cleaved at a rate of 1.5×10^{-4} min^{-1} (Kuimelis & McLaughlin, 1995a), which is roughly 1 million-fold faster than estimates for the spontaneous cleavage of native oxo linkages in dinucleoside monophosphates (Milstein & Fife, 1967; Nakamaye et al., 1988; Shapiro & Vallee, 1989; Komiyama et al., 1992). Not unexpectedly, divalent metals were observed to increase the cleavage rates by 10−5000-fold (Table 1). Our initial studies on the influence of divalent metals upon the cleavage rate were performed at both 5 and 10 mM metal, and the cleavage rates did not vary at these two concentrations. In both cases, the divalent metal is in vast excess (at least 10^6-fold) over the thio linkage. Neither the oxo analogue (i.e., sequence **1**, containing a single ribonucleotide at C_{17}) nor the all-deoxy bridging 5′-phosphorothioate underwent any detectable cleavage in the absence of ribozyme under the conditions and times examined [see Kuimelis and McLaughlin (1995a)]. These observations underscore the importance of the participating 2′-hydroxyl adjacent to the bridging 5′-phosphorothioate in the

[1] The pK_a of methanol is 15.5 vs 10.0 for methanethiol (Dean, 1985).

Table 1: Cleavage Rates of the Phosphorothioate Analogue with Divalent Metals

	k_{obs} (min^{-1})				
metal	control[a]	ribozyme[b]	ribozyme + spermine[c]	pK_a[d]	radius (Å)[e]
EDTA	0.00015	0.00012	0.023	–	–
Mg^{2+}	0.0015	0.065 (0.035)	0.093 (0.045)	11.4	0.65
Ca^{2+}	0.0037	0.045	0.066	12.8	0.99
Mn^{2+}	0.011	0.082 (0.097)	0.083 (0.15)	10.6	0.80
Co^{2+}	0.015	0.024	0.039	9.9	0.74
Zn^{2+}	0.057	0.013	0.025	9.0	0.74
Cd^{2+}	0.53	0.15	0.29	9.0	0.97

[a] 5 mM metal dichloride or EDTA and 50 mM Tris-HCl (pH 7.5). [b] 0.5 μM ribozyme, 10 mM metal dichloride, and 50 mM Tris-HCl (pH 7.5). Values in parentheses are for cleavage of the oxo substrate, **1**. [c] 0.5 mM spermine added to the ribozyme reaction mixture. Values in parentheses are for cleavage of the oxo substrate, **1**. [d] Acid dissociation constants for hydrated metal cations at 25 °C are from Dean (1985). Standard deviations for the reported rate constants are less than ±10% (see Materials and Methods). [e] Ionic radii are from Dean (1985).

cleavage mechanism. A detailed investigation of the chemical cleavage properties of the bridging 5′-phosphorothioate has appeared elsewhere (Kuimelis & McLaughlin, 1995a).

In the presence of excess ribozyme (1000-fold) and 10 mM Mg^{2+} at pH 7.5, the cleavage rate of the phosphorothioate substrate is increased 540-fold to 0.065 min^{-1} (compare with 1.2×10^{-4} min^{-1}; see Table 1). In the absence of ribozyme, Mg^{2+} only increases the cleavage rate 10-fold. Mn^{2+} stimulates the ribozyme-promoted cleavage of the phosphorothioate 680-fold, but the control rate is only increased 70-fold by this metal. The increased control rate for the phosphorothioate substrate (i.e., no ribozyme) with Mn^{2+} relative to that with Mg^{2+} is consistent with its "softer" character and greater affinity for sulfur (Huheey, 1983; Pearson, 1990, 1993). By comparison, the oxo substrate was cleaved with rates of 0.035 and 0.097 min^{-1} in 10 mM Mg^{2+} and Mn^{2+}, respectively (see Table 1).

Several other divalent metals were also tested for their ability to facilitate the ribozyme-promoted cleavage of the thio substrate: Ca^{2+}, Co^{2+}, Zn^{2+}, and Cd^{2+}. Ca^{2+} was fairly effective at promoting cleavage (0.045 min^{-1}) but less so than Mg^{2+} or Mn^{2+}. Surprisingly, the ribozyme-promoted cleavage rates of the phosphorothioate substrate in the presence of Zn^{2+} or Cd^{2+} (0.013 and 0.15 min^{-1}) were substantially lower than the control rates in the absence of ribozyme (0.057 and 0.53 min^{-1}). In these cases, the ribozyme−substrate complex actually affords moderate protection from cleavage. This observation suggests that the ribozyme does not effectively bind Zn^{2+} or Cd^{2+} and use them as efficient catalytic cofactors. Moreover, these results imply that the labile bridging 5′-phosphorothioate linkage is somewhat shielded from the bulk solution by the tertiary structure of the folded ribozyme−substrate complex.

No correlation exists between the ribozyme-promoted cleavage of the thio analogue and the acid dissociation constants (pK_as) of the hydrated metal cations (see Table 1). For example, the pK_as of Zn^{2+} and Cd^{2+} are quite similar at 9.0 (Dean, 1985), but the cleavage rates differ by 1 order of magnitude. Additionally, the p*K*a of Ca^{2+} is 2.2 units greater than that of Mn^{2+} (12.8 vs 10.6), but the Mn^{2+}-catalyzed cleavage rate is less than 2-fold greater than that of Ca^{2+}. These observations suggest that the role of the divalent metal cofactor is more than that of a general base to facilitate deprotonation of the attacking 2′-hydroxyl group and may reflect the geometric constraints of a metal binding pocket or the different ligand preferences of the various metals. The ionic radii of the divalent metals listed in Table 1 range from 0.65 to 0.97 Å (Dean, 1985), but no relationship emerges and there does not appear to be a requirement for a particular size within this range.

Clearly, the lack of a distinct preference for a particular metal cofactor in the ribozyme/thio analogue complex, and in particular the similarity of the cleavage rates in the presence of Mg^{2+} or Mn^{2+}, provides strong evidence that the metal cofactor does not interact with the 5′-thioanion (or 5′-oxyanion) leaving group in the transition state (Kuimelis & McLaughlin, 1995b). Determinations of the affinity of divalent metals for ATPβS reveal that Mg^{2+} is coordinated 30 000 times more strongly to oxygen than to sulfur, whereas Mn^{2+} binds the two ligands almost equally (Jaffe & Cohn, 1978; Pecoraro et al., 1984). If the metal cofactor interacted with the leaving group in the transition state, then substantial rate differences would be expected between the two metals. Using a nonbridging phosphorothioate at the hammerhead ribozyme cleavage site, the *pro*-R oxygen has been implicated as a metal ligand based on the basis of its influence on the cleavage rate (Dahm & Uhlenbeck, 1991; Koizumi & Ohtsuka, 1991; Slim & Gait, 1991). In the case of the *Tetrahymena* ribozyme (group I intron), where the 3′-oxygen is the leaving group, replacement of the 3′-bridging phosphate oxygen with a sulfur atom in an all-deoxy substrate resulted in a 1000-fold rate differential for Mn^{2+} vs Mg^{2+}, clearly establishing that the metal cofactor participates in the first cleavage reaction by associating with the 3′-leaving group as a Lewis acid (Piccirilli et al., 1993). In contrast, the lack of a preference for Mn^{2+} vs Mg^{2+} in the hammerhead ribozyme-mediated cleavage of the 5′-bridging phosphorothioate provides compelling evidence that a metal cofactor does not interact with the 5′-leaving group in the transition state and therefore that the proposed double-metal mechanism (Steitz & Steitz, 1993; Sawata et al., 1995) does not appear to be applicable to the hammerhead ribozyme.

Effect of Spermine. The polyamine spermine is known to stabilize higher-order nucleic acid structures at low millimolar concentrations (Saenger, 1983), and it has been previously employed in the hammerhead system in an effort to separate the possible structure-stabilizing role of the divalent metal from the possible catalytic role (Dahm & Uhlenbeck, 1991). As revealed in Table 1, the addition of 0.5 mM spermine to the ribozyme reaction mixture had the general effect of increasing the cleavage rates by about 0.02 min^{-1}. Spermine also increased the rate of cleavage of the oxo substrate by roughly the same amount in the presence of either Mg^{2+} or Mn^{2+}. Remarkably, in the complete absence of divalent metals (5 mM EDTA), spermine alone increased the ribozyme-promoted cleavage of the bridging 5′-phosphorothioate nearly 200-fold to 0.023 min^{-1}, a value which is comparable to the metal-assisted cleavage rates (see Table 2). In contrast, the oxo substrate did not undergo any detectable ribozyme-promoted cleavage in the presence of EDTA and spermine. To investigate further the apparent ability of spermine to replace the metal cofactor in the thio analogue−ribozyme complex, we examined the effect of the closely related polycation spermidine, which has one less aminopropyl group. Spermidine, like spermine, is also

Table 2: Cleavage Rates of the Oxo and Phosphorothioate Analogue with Cations

	oxo	thio	
cation	k_{obs} (min^{-1})	k_{obs} (min^{-1})	k_{rel}
Mg^{2+} (10 mM)	0.035	0.065	1.8
spermine (0.5 mM)[a]	nd[b]	0.023	0.7
spermidine (0.5 mM)[a]	nd	nd	−
NaCl (0.5 M)[a]	nd	nd	−

[a] Reaction mixtures also contained 5 mM EDTA. [b] nd = no detectable cleavage observed ($< 1.0 \times 10^{-5}$ min^{-1}). Standard deviations are ±10%.

known to stabilize higher-order nucleic acid structures at low millimolar concentrations. However, neither the oxo nor the thio substrate underwent detectable ribozyme-promoted cleavage in the presence of 0.5 mM spermidine and 5 mM EDTA. NaCl is also capable of stabilizing nucleic acid duplexes and higher-order structures, albeit at a much higher concentration, but 500 mM NaCl did not cause any detectable ribozyme-promoted cleavage of either substrate in the absence of a divalent metal (see Table 2). These data suggest a special role for spermine beyond the simple organization of the proper complex conformation. It is possible that the spermine molecule actually participates in the cleavage reaction by orienting itself in the folded complex and functioning as a general acid or base to facilitate the cleavage event, perhaps reminiscent of the role of the histidine residue(s) in the RNAse A reaction (Deakyne & Allen, 1979). tRNAs that are crystallized in the presence of spermine reveal specifically bound spermine molecules (Holbrook et al., 1978; Quigley et al., 1978; Stout et al., 1978) that reside in the helical regions and bridge intrahelical phosphate moieties; similar binding may occur in the catalytically competent hammerhead ribozyme. The fact that spermidine does not promote cleavage may reflect a specific chain length requirement for binding and/or catalysis. The precise role of the spermine remains to be established through additional experimentation.

pH Experiments. In the presence of Mg^{2+} or Mn^{2+}, the oxo substrate exhibits a linear pH vs rate profile in the range of pH 6.0−8.0. The rate decreases above pH 8.0, possibly due to the formation of metal oxides. The slopes of the linear portions of the lines are 1.1 and 0.78 for Mg^{2+} or Mn^{2+}, respectively. Similar values were obtained for native, all-ribo substrates (Dahm et al., 1993). A linear pH rate profile provides strong evidence that the chemical cleavage step, as opposed to a conformational change, is the rate-determining step. The thio analogue also exhibits a linear pH vs rate profile between pH 6.5 and 8.5 in the presence of Mg^{2+} or Mn^{2+} (see Figure 6). The slopes of the lines are 0.36 and 0.24 for Mg^{2+} and Mn^{2+}, respectively. Although the slopes of the lines are lower for the thio analogue, this may be due to the leveling off of the curve at the lowest pH values. Qualitatively, comparison of the pH vs rate profiles for the oxo and thio substrates reveals that for both substrates the linear portions of the lines for Mg^{2+} and Mn^{2+} intersect at pH 8.5, and in both cases, Mn^{2+} gives the smaller slope.

Metal Concentration Experiments. Figure 7 illustrates the effect of Mg^{2+} concentration on the ribozyme-promoted cleavage rates of the oxo and thio substrates. These experiments were performed at pH 7.5 in the linear portion of the pH vs rate profile (see above). The Mg^{2+} curves indicate cooperative metal binding with saturation near 100

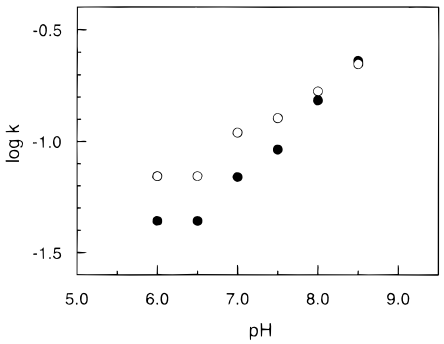

FIGURE 6: Hammerhead ribozyme-mediated cleavage rates for the thio analogue **2** as a function of pH in the presence of (●) Mg^{2+} or (○) Mn^{2+}.

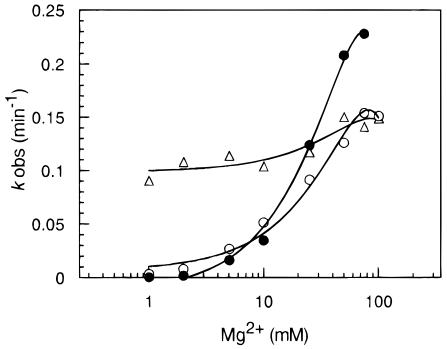

FIGURE 7: Hammerhead ribozyme-mediated cleavage rates as a function of Mg^{2+} concentration: (●) oxo analogue **1**, (○) thio analogue **2**, and (△) thio analogue **2** with 0.5 mM spermine.

mM. In the case of Mn^{2+}, it was not possible to use concentrations greater than about 10 mM without progressive reductions in the cleavage rate, possibly due to precipitation of metal hydroxides at the higher concentrations (Dahm et al., 1993). Comparison of the metal saturation curves for the oxo and thio substrates reveals strong similarities with regard to the concentrations required for saturation (in the absence of spermine) and the apparent dissociation constants for the divalent metal (see supporting information). This suggests that both the oxo and thio substrate−ribozyme complexes interact with the divalent metal in a similar fashion. In the absence of spermine, the cleavage rate of the thio substrate ranged from 0.002 to 0.15 min^{-1} at concentrations of 1−100 mM Mg^{2+}. The oxo substrate was cleaved at rates between 0.000 34 and 0.23 min^{-1} over the same concentration range. The effect of spermine on the metal concentration curve for the oxo substrate was to broaden the transition, particularly with Mn^{2+} (see supporting information). This effect has been observed previously by Uhlenbeck and co-workers (Dahm & Uhlenbeck, 1991). Figure 7 also reveals that, in the presence of 0.5 mM spermine, the divalent metal concentration has very little effect on the ribozyme-promoted cleavage of the thio substrate; rate constants range from 0.090 to 0.14 min^{-1} between 1 and 100 mM Mg^{2+}, less than a 2-fold rate increase. Indeed, even in the complete absence of a divalent metal (5 mM EDTA), the cleavage rate of the thio substrate was 0.023 min^{-1} when spermine was present in the reaction mixture.

Temperature Experiments. The influence of the reaction temperature on the ribozyme-promoted cleavage of both the oxo linkage and the thio analogue was examined by measurement of the rate of cleavage at temperatures between 0 and 50 °C in the presence of either Mg^{2+} or Mn^{2+} at pH

Table 3: Cleavage Rates of the Oxo Linkage in Deuterium Oxide[a]

	no spermine		spermine (0.5 mM)	
solvent	k_{obs} (min^{-1})	k_{obs}/k_{D_2O}	k_{obs} (min^{-1})	k_{obs}/k_{D_2O}
H_2O	0.035	3.6	0.047	2.3
H_2O/D_2O	0.018	1.8	0.031	1.5
D_2O	0.010	1.0	0.021	1.0

[a] Standard deviations are ±10%.

7.5. The effect of temperature on the cleavage of the thio analogue in the presence of EDTA and spermine was also determined. As expected, the cleavage rates increase linearly as the reaction temperature is elevated from 0 to 30 °C (see supporting information). In the case of the oxo linkage, the cleavage rate drops sharply at temperatures above about 30 °C due to the melting out of the tertiary structure required for catalysis or to the decrease in the fraction of substrate that is bound. It is difficult to obtain reliable activation energies from this complex due to both the low T_m (helix−coil transition), which limits the number of data points that can be collected between the T_m and the freezing point of the aqueous reaction mixture, and the apparent small activation energy itself (3.5 and 2.8 kcal mol^{-1} for Mg^{2+} and Mn^{2+}, respectively). In any event, the activation energy obtained for the oxo linkage in the presence of either Mg^{2+} or Mn^{2+} is quite similar.

The effect of temperature on the ribozyme-promoted cleavage of the thio analogue in the presence of either Mg^{2+} or Mn^{2+} is not as pronounced as that of the oxo linkage. This is due to the metal-assisted, chemical (non-ribozyme) cleavage of the displaced substrate strand at the elevated temperatures and reflects the protection that is afforded to the phosphorothioate linkage in the folded ribozyme−substrate complex. If spermine is used in place of the divalent metal and EDTA is also present in the reaction mixture, the chemical cleavage can be minimized by elimination of the metal-assisted cleavage in the uncomplexed state, and the dramatic drop in rate at the higher temperatures is restored. Reliable activation energies for the thio analogue could not be obtained for the reasons described above, but comparison of the graphs revealed that the activation energy for cleavage of the thio linkage appears to be slightly smaller than that for the oxo linkage (see supporting information).

Solvent Isotope Effect Experiments. Ribozyme reactions were conducted in deuterium oxide as solvent to investigate the possibility of proton transfer processes in the rate-determining step of the cleavage mechanism. At some point in the reaction pathway, the 2′-hydroxyl at C_{17} and the 5′-oxyanion (or thioanion) at $A_{1.1}$ must undergo deprotonation and protonation, respectively. Either process could lead to a solvent isotope effect if either of the proton transfers takes place at the rate-determining step. Thus, the cleavage reactions were carried out both in pure D_2O and in a 1:1 H_2O/D_2O mixture at pH 7.5. The results are summarized in Table 3. The oxo linkage exhibited a solvent deuterium isotope effect (k_H/k_D) of 3.6 in the presence of a Mg^{2+} cofactor, and the isotope effect in the 1:1 D_2O/H_2O mixture was an intermediate value of 1.8. Similar results were recently reported for the hammerhead ribozyme-promoted cleavage of an all-ribo substrate, although a different ribozyme sequence was employed and the reactions were performed at pH 6.0 as opposed to pH 7.5 (Sawata et al., 1995b). These authors attributed the observed isotope effect ($k_H/k_D = 4.4$) solely to a decrease in the amount of the metal deuteroxide moiety (e.g., $[M(OD)]^{1+}$) as a result of the altered equilibrium constant in D_2O vs H_2O solvent. Metal hydroxide has been implicated as the active species which deprotonates the 2′-hydroxyl to initiate cleavage in the hammerhead ribozyme on the basis of pH rate profiles with various divalent metals (Dahm et al., 1993). It remains to be determined if the observed solvent isotope effects represent an actual proton transfer or simply a decrease in the concentration of the postulated active metal species.

As shown in Table 3, the influence of spermine on the solvent deuterium isotope effect was to decrease its magnitude from 3.6 to 2.3. It is unlikely that 0.5 mM spermine alters the equilibrium constant of the postulated active metal species, so it is probable that the spermine perturbs the transition state structure to affect this change. It is not clear if the spermine acts near the cleavage site or at some other location further removed. In any event, the role of spermine seems to be to diminish or relieve the importance of the divalent metal cofactor. This is consistent with our finding that the thio analogue is efficiently cleaved by the hammerhead ribozyme in the complete absence of a divalent metal cofactor, provided spermine is present in the reaction mixture.

Unlike the oxo linkage, the thio analogue did not exhibit a measurable solvent deuterium isotope effect in the presence of either Mg^{2+} or spermine and EDTA. One interpretation of the lack of a solvent isotope effect for the thio analogue is that the cleavage mechanism has been distinctly altered by replacement of the oxygen atom with a sulfur atom, such that a different step in the cleavage process is now rate-limiting, one that does not involve a proton transfer. More subtly, the lack of a solvent isotope effect for the thio analogue could also represent a slight perturbation of the transition state along the reaction coordinate, thus decreasing the influence of a proton transfer process on the reaction rate. Because in almost every other respect the thio analogue behaves kinetically very much like the oxo linkage, we believe that the latter interpretation is more appropriate.

CONCLUSION

Replacing the bridging 5′-oxygen atom of a native RNA phosphodiester linkage with a 5′-sulfur atom enhances the leaving group ability of the 5′-substituent and labilizes the specific phosphorus−heteroatom bond that is broken during the hammerhead ribozyme-catalyzed transesterification reaction. In the absence of ribozyme or a divalent metal, the bridging 5′-phosphorothioate linkage is about 1 million-fold more labile than the native ribo phosphodiester, which is consistent with the known pK_a differences between the hydroxy and thiol moieties. Divalent metals dramatically accelerate the chemical cleavage rate, apparently by functioning as Lewis acids to assist in the neutralization of the developing negative charge on the 5′-thio group (Kuimelis & McLaughlin, 1995a). In spite of the greatly enhanced lability of this modified linkage, the substrate analogue containing a 5′-bridging phosphorothioate diester exhibits hammerhead ribozyme-catalyzed cleavage kinetics that are virtually identical to those observed for the native oxo linkage. This comparison suggests that the bond-breaking event involving departure of the 5′-leaving group is not the

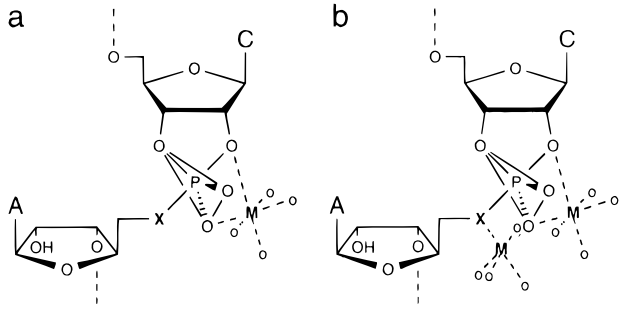

FIGURE 8: Transition state of the hammerhead ribozyme illustrating (a) the single-metal model and (b) the double-metal model. The ○ symbols represent undefined ligands or H_2O.

rate-limiting step of the cleavage reaction, and a two-step mechanism must be invoked to accommodate this observation. It then follows that one of the first steps of the transesterification reaction pathway, deprotonation of the 2′-hydroxyl or nucleophilic attack on the scissile phosphodiester, must be rate-limiting. The lack of a preference for the "soft" Mn^{2+} cofactor over the "hard" Mg^{2+} cofactor implies that the divalent metal does not interact with the 5′-sulfur (or oxygen) leaving group in the transition state (Kuimelis & McLaughlin, 1995b). These observations do not support a previously proposed double-metal mechanism for the hammerhead ribozyme (Steitz & Steitz, 1993; Sawata et al., 1995), where the second metal associates with the 5′-leaving group and helps to facilitate catalysis by functioning as a Lewis acid (compare panels a and b Figure 8). However, it is clear that in other phosphoryl transfer reactions a metal cofactor does in fact serve this role (Freemont et al., 1988; Beese & Steitz, 1991; Piccirilli et al., 1993). Spermine appears to be capable of properly organizing the ribozyme catalytic domain, and with a suitably labile linkage (the 5′-bridging phosphorothioate), cleavage proceeds efficiently in the complete absence of a divalent metal cofactor.

Primarily deoxy substrates behave very much like the corresponding all-ribo substrates with regard to their cleavage by the hammerhead ribozyme, and many of the experiments described here with oligomer **1** go further to support this fact. We have additionally demonstrated through extensive characterization that the phosphorothioate substrate **2** behaves very much like the control substrate, **1**. On a purely structural level, it should be pointed out that DNA/RNA heteroduplexes adopt the A-type duplex that is found in RNA/RNA homoduplexes, although minor perturbations likely exist (Saenger, 1983; Hall & McLaughlin, 1991). Two recently solved X-ray structures of hammerhead ribozyme−inhibitor complexes, one employing an all-DNA substrate and another employing an all-RNA substrate, give virtually identical three-dimensional structures (Pley et al., 1994; Scott et al., 1995). Thus, there is good precedent, and it is valid to extrapolate the results from our simplified, primarily deoxy substrates (oxo and thio) to the native, all-ribo substrate. The kinetic data that we have obtained with the bridging 5′-phosphorothioate substrate analogue are consistent with a hammerhead cleavage mechanism involving only a single critical metal cofactor that is either required by the ribozyme to deprotonate the active site 2′-hydroxyl or is necessary in some other fashion to facilitate nucleophilic attack by the 2′-hydroxyl on the scissile phosphodiester. Such a single-metal mechanism would be consistent with the well-established mechanism for the nonbiological, Pb^{2+}-mediated cleavage of tRNA (Marciniec et al., 1989; Behlen et al., 1990). Using X-ray crystallographic analysis of a hammerhead ribozyme−inhibitor complex, Scott et al. have identified a Mg^{2+} atom near the active site and have proposed a single-metal mechanism for the hammerhead ribozyme cleavage reaction that is in general agreement with our findings (Scott et al., 1995).

SUPPORTING INFORMATION AVAILABLE

pH rate profile for the ribozyme-mediated cleavage of the oxo analogue (**1**); metal concentration rate profiles for the ribozyme-mediated cleavage of the oxo (**1**) and thio (**2**) analogues in the presence of Mn^{2+} or Mn^{2+}/spermine; and temperature rate profile for the ribozyme-mediated cleavage of the oxo (**1**) and thio (**2**) analogues in the presence of Mg^{2+}, Mn^{2+}, or spermine/EDTA (6 pages). Ordering information is given on any current masthead page.

REFERENCES

Almer, H., & Strömberg, R. (1991a) *Tetrahedron Lett. 32*, 3723−3726.

Almer, H., & Strömberg, R. (1991b) *Nucleosides Nucleotides 10*, 653−655.

Beese, L. S., & Steitz, T. A. (1991) *EMBO J. 10*, 25−33.

Behlen, L. S., Sampson, J. R., DiRenzo, A. B., & Uhlenbeck, O. C. (1990) *Biochemistry 29*, 2515−2523.

Dahm, S. C., & Uhlenbeck, O. C. (1990) *Biochimie 72*, 819−823.

Dahm, S. C., & Uhlenbeck, O. C. (1991) *Biochemistry 30*, 9464−9469.

Dahm, S. C., Derrick, W. B., & Uhlenbeck, O. C. (1993) *Biochemistry 32*, 13040−13045.

Deakyne, C. A., & Allen, L. C. (1979) *J. Am. Chem. Soc. 101*, 3951−3959.

Dean, J. A. (1985) *Lange's Handbook of Chemistry*, 13th ed., McGraw-Hill, New York.

Forster, A. C., & Symons, R. H. (1987) *Cell 50*, 9−16.

Freemont, P. S., Friedman, J. M., Beese, L. S., Sanderson, M. R., & Steitz, T. A. (1988) *Proc. Natl. Acad. Sci. U.S.A. 85*, 8924−8928.

Fu, D. J., & McLaughlin, L. W. (1992) *Biochemistry 31*, 10941−10949.

Gasparutto, D., Livache, T., Bazin, H., Duplaa, A.-M., Guy, A., Khorlin, A., Molko, D., Roget, A., & Teoule, R. (1992) *Nucleic Acids Res. 20*, 5159−5166.

Hall, K. B., & McLaughlin, L. W. (1991) *Biochemistry 30*, 10606−10613.

Hertel, K. J., & Uhlenbeck, O. C. (1995) *Biochemistry 34*, 1744−1749.

Hertel, K. J., Herschlag, D., & Uhlenbeck, O. C. (1994) *Biochemistry 33*, 3374−3385.

Heus, H. A., & Pardi, A. (1991) *J. Mol. Biol. 217*, 113−124.

Hodgson, R. A. J., Shirley, N. J., & Symons, R. H. (1994) *Nucleic Acids Res. 22*, 1620−1625.

Holbrook, S. R., Sussman, J. L., Warrant, R. W., & Kim, S.-H. (1978) *J. Mol. Biol. 123*, 631−660.

Huheey, J. E. (1983) *Inorganic chemistry: principles of structure and reactivity*, Harper and Row, New York.

Jaffe, E. K., & Cohn, M. (1978) *J. Biol. Chem. 253*, 4823−4825.

Jeoung, Y. H., Kumar, P. K. R., Suh, Y. A., Taira, K., & Nishikawa, S. (1994) *Nucleic Acids Res. 22*, 3722−3727.

Koizumi, M., & Ohtsuka, E. (1991) *Biochemistry 30*, 5145−5150.

Komiyama, M., Matsumura, K., & Matsumoto, Y. (1992) *J. Chem. Soc., Chem. Commun.*, 640−641.

Kuimelis, R. G., & McLaughlin, L. W. (1995a) *Nucleic Acids Res. 23*, 4753−4760.

Kuimelis, R. G., & McLaughlin, L. W. (1995b) *J. Am. Chem. Soc. 117*, 11019−11020.

Kuimelis, R. G., & McLaughlin, L. W. (1996) in *Nucleic Acids and Molecular Biology* (Eckstein, F., Ed.) Vol. 10, Springer-Verlag, Berlin (in press).

Long, D. M., & Uhlenbeck, O. C. (1994) *Proc. Natl. Acad. Sci. U.S.A. 91*, 6977−6981.
Marciniec, T., Ciesiolka, J., Wrzesinski, J., & Wlodzimierz, K. J. (1989) *FEBS Lett. 243*, 293−298.
Matteucci, M. D., & Caruthers, M. H. (1981) *J. Am. Chem. Soc. 103*, 3185−3191.
Milstein, S., & Fife, T. H. (1967) *J. Am. Chem. Soc. 89*, 5820−5826.
Nakamaye, K. L., Gish, G., & Eckstein, F. (1988) *Nucleic Acids Res. 16*, 9947−9958.
Pearson, R. G. (1990) *Coord. Chem. Rev. 100*, 403−425.
Pearson, R. G. (1993) *Acc. Chem. Res. 26*, 250−255.
Pecoraro, V. L., Hermes, J. D., & Clelend, W. W. (1984) *Biochemistry 23*, 5262−5271.
Pentz, L., & Thornton, E. R. (1967) *J. Am. Chem. Soc. 89*, 6931−6938.
Perreault, J.-P., Wu, T.-F., Cousineau, B., Ogilvie, K. K., & Cedergren, R. (1990) *Nature 344*, 565−567.
Perreault, J.-P., Labuda, D., Usman, N., Yang, J. H., & Cedergren, R. (1991) *Biochemistry 30*, 4020−4025.
Piccirilli, J. A., Vyle, J. S., Caruthers, M. H., & Cech, T. R. (1993) *Nature 361*, 85−88.
Pley, H. W., Flaherty, K. M., & McKay, D. B. (1994) *Nature 372*, 68−74.
Pyle, A. M. (1993) *Science 261*, 709−714.
Quigley, G. J., Teeter, M. M., & Rich, A. (1978) *Proc. Natl. Acad. Sci. U.S.A. 75*, 64−68.
Ruffner, D. E., Stormo, G. D., & Uhlenbeck, O. C. (1990) *Biochemistry 29*, 10695−10702.
Saenger, W. (1983) *Principles of nucleic acid structure*, Springer-Verlag, New York.
Sakatsume, O., Ogawa, T., Hosaka, H., Kawashima, M., Takaki, M., & Takaku, H. (1991a) *Nucleosides Nucleotides 10*, 141−153.
Sakatsume, O., Yamaguchi, T., Ishikawa, M., Hirao, I., Miura, K.-i., & Takaku, H. (1991b) *Tetrahedron 47*, 8717−8728.
Sawata, S., Komiyama, M., & Taira, K. (1995) *J. Am. Chem. Soc. 117*, 2357−2358.
Scott, W. G., Finch, J. T., & Klug, A. (1995) *Cell 81*, 991−1002.
Shapiro, R., & Vallee, B. L. (1989) *Biochemistry 28*, 7401−7408.
Slim, G., & Gait, M. J. (1991) *Nucleic Acids Res. 19*, 1183−1188.
Steitz, T. A., & Steitz, J. A. (1993) *Proc. Natl. Acad. Sci. U.S.A. 90*, 6498−6502.
Stout, C. D., Mizuno, H., Rao, S. T., Swaminathan, P., Rubin, J., Brennan, T., & Sundaralingam, M. (1978) *Acta Crystallogr. B 34*, 1529−1544.
Symons, R. H. (1989) *TIBS 14*, 445−450.
Symons, R. H. (1991) *Crit. Rev. Plant Sci. 10*, 189−234.
Taira, K., Uebayasi, M., Maeda, H., & Furukawa, K. (1990) *Protein Eng. 3*, 691−701.
Taira, K., Uchimaru, T., Tanabe, K., Uebayasi, M., & Nishikawa, S. (1991) *Nucleic Acids Res. 19*, 2747−2753.
Tuschl, T., Gohlke, C., Jovin, T. M., Westhof, E., & Eckstein, F. (1994) *Science 266*, 785−789.
Uebayasi, M., Uchimaru, T., Koguma, T., Sawata, S., Shimayama, T., & Taira, K. (1994) *J. Org. Chem. 59*, 7414−7420.
Uhlenbeck, O. C. (1987) *Nature 321*, 596−600.
Usman, N., Ogilvie, K. K., Jiang, M.-Y., & Cedergren, R. J. (1987) *J. Am. Chem. Soc. 109*, 7845.
van Tol, H., Buzayan, J. M., Feldstein, P. A., Eckstein, F., & Bruening, G. (1990) *Nucleic Acids Res. 18*, 1971−1975.
Westman, E., & Strömberg, R. (1994) *Nucleic Acids Res. 22*, 2430−2431.
Yamakage, S.-i., Sakatsume, O., Furuyama, E., & Takaku, H. (1989) *Tetrahedron Lett. 30*, 6361−6364.
Yang, J. H., Perreault, J. P., Labuda, D., Usman, N., & Cedergren, R. (1990) *Biochemistry 29*, 11156−11160.
Yang, J. H., Usman, N., Chartrand, P., & Cedergren, R. (1992) *Biochemistry 31*, 5005−5009.
Yarus, M. (1993) *FAESB J. 7*, 31−39.

BI952994P